

Ferroelectric Properties of $\text{Bi}_4\text{Ti}_3\text{O}_{12}$ Thin Films with TiO_2 Anatase Layer on Pt/Ti/SiO₂/Si Substrates Prepared by MOCVD

Mitsuru Konishi, Tohru Higuchi, Yuji Hachisu, Makoto Nakamura, Takeshi Hattori
and Takeyo Tsukamoto

Department of Applied Physics, Tokyo University of Science, 1-3 Kagurazaka, Shinjuku, Tokyo 162-8601, Japan
Fax: 81-3-5228-8241, e-mail: higuchi@rs.kagu.tus.ac.jp

$\text{Bi}_4\text{Ti}_3\text{O}_{12}$ (BIT) thin films with TiO_2 anatase layer have been prepared on the Pt/Ti/SiO₂/Si substrates by metalorganic vapor deposition. The BIT thin films with TiO_2 anatase buffer layer exhibit highly a- and b-axes orientation, although the BIT thin film with no buffer layer exhibits a c-axis orientation. The ferroelectricity depends on the thickness ratio of the BIT thin film to the TiO_2 anatase layer, indicating that the TiO_2 anatase buffer layer acts not as barrier layer but as an initial nucleation layer. When the thickness ratio is fixed at $[(\text{BIT})/(\text{TiO}_2)] = 15$, the remanent polarization (P_r) and the coercive field (E_c) are $2P_r = 81.6 \mu\text{C}/\text{cm}^2$ and $2E_c = 250 \text{ kV}/\text{cm}$, respectively. The dielectric constant (ϵ_r) is 160.

Key words: MOCVD, $\text{Bi}_4\text{Ti}_3\text{O}_{12}$ (BIT), TiO_2 anatase, interface, initial nucleation, remanent polarization (P_r)

1. INTRODUCTION

Ferroelectric $\text{Bi}_4\text{Ti}_3\text{O}_{12}$ (BIT) has been expected to be applied to nonvolatile ferroelectric random access memories (FeRAMs) with nondestructive readout operation, because of its low dielectric constant and coercive field [1-4]. The BIT thin films are useful lead-free and fatigue-free ferroelectric materials that exhibit superior ferroelectricity even when using Pt electrodes. The large P_r of the a-axis takes advantage of the reduction of the memory cell area of a NV-FeRAM. The formation process at low temperature below 500 °C is desirable for the realization of poly-Si-plug-stacked capacitor memory cells [5-12]. This is because interdiffusion occurs between the electrode and the poly-Si-plug during ferroelectric film formation at high temperature.

In recent years, the $\text{Bi}_{4-x}\text{La}_x\text{Ti}_3\text{O}_{12}$ thin film, which was prepared at a crystallization temperature of 650°C, exhibited a relatively large remanent polarization, and superior fatigue endurance was confirmed [4-6]. Such a significant improvement in ferroelectricity has been observed only for $(\text{Bi}_{4-x}\text{La}_x)(\text{Ti}_{3-y}\text{V}_y)\text{O}_{12}$ and $\text{Bi}_4\text{Ti}_{3-y}\text{V}_y\text{O}_{12}$ films [19-22]. Matsuda *et al.* prepared a Pr-substituted BIT ($\text{Bi}_{4-x}\text{Pr}_x\text{Ti}_3\text{O}_{12}$) thin film grown on an Ir/Si substrate from chemical solution [23]. They reported that the polar-axis-oriented $\text{Bi}_{3.7}\text{Pr}_{0.3}\text{Ti}_3\text{O}_{12}$ thin film has the remanent polarization (P_r) of $2P_r = 92 \mu\text{C}/\text{cm}^2$. However, these BIT thin films require high crystallization temperatures above 600°C.

In this study, the a- and b-axes-oriented BIT thin films have been prepared on Pt/Ti/SiO₂/Si substrates by MOCVD using $\text{Bi}(\text{CH}_3)_3$ and $\text{Ti}(i\text{-OCH}_3\text{H}_7)_4$ sources. In order to prevent the interdiffusion, the TiO_2 anatase buffer layer is inserted between the BIT thin film and Pt/Ti/SiO₂/Si substrate [14,15]. TiO_2 anatase can be prepared at a low substrate temperature of 350°C by MOCVD [14,26,27]. Thus, the TiO_2 anatase buffer layer is very effective for inducing interdiffusion between the BIT thin film and the Pt substrate. In this

paper, we present the structural and ferroelectric properties of the BIT thin films with a TiO_2 anatase buffer layer.

2. EXPERIMENTAL

TiO_2 anatase buffer layers were prepared on (111) Pt/Ti/SiO₂/Si substrates by MOCVD. Tetra-isopropoxy titanium [$\text{Ti}(i\text{-OCH}_3\text{H}_7)_4$] was used as the Ti source in MOCVD. The pressure in the reaction chamber was fixed at approximately 5 Torr. $\text{Ti}(i\text{-OCH}_3\text{H}_7)_4$ was vaporized in a separate stainless-steel bubbler and maintained at 40°C. The substrate temperature (T_s) was approximately 350°C [14,26,27]. The prepared TiO_2 anatase film exhibited (101) orientation.

BIT thin films were deposited by MOCVD on the TiO_2 anatase buffer layer prepared on Pt/Ti/SiO₂/Si substrates, using an apparatus having a vertical cold-wall reaction chamber. Trimethyl bismuth [$\text{Bi}(\text{CH}_3)_3$] and $\text{Ti}(i\text{-OCH}_3\text{H}_7)_4$ were used as Bi and Ti sources in MOCVD. The $\text{Bi}(\text{CH}_3)_3$ and $\text{Ti}(i\text{-OCH}_3\text{H}_7)_4$ were vaporized in separate stainless-steel bubblers and maintained at 0°C and 40°C, respectively. The Ar and O₂ gases were used as the carrier gas and the oxidizing gas, respectively. The pressure in the reaction chamber was fixed at approximately 5 Torr [12,13]. The substrate temperature (T_{sub}) was fixed at 500°C. Finally, the top Pt electrodes with a diameter of 0.2 mm were deposited on the film surface through a metal shadow mask by rf-magnetron sputtering in order to measure the electrical properties.

The structural properties of the BIT thin films were characterized by X-ray diffraction (XRD) using CuK α . The surface morphology and cross section were observed by scanning electron microscopy (SEM). The electrical properties were measured using the ferroelectric property measurement system.

3. RESULTS AND DISCUSSION

Figure 1 shows the XRD patterns of as-deposited BIT thin films with the TiO_2 anatase buffer layer and with no buffer layer. The T_{sub} and deposition pressure of these thin films were fixed at 500°C and 5 Torr, respectively. The thicknesses of the buffer layer and BIT thin film were fixed at 50 nm and 350 nm, respectively. The compositional ratio of Bi and Ti was almost stoichiometrical in these films. The XRD pattern of the BIT thin film with no buffer layer exhibits a highly c -axis-oriented BIT single phase, although the (111) and (117) peaks are observed at $2\theta \sim 23.4^\circ$ and 30.0° , respectively. The XRD pattern of the BIT thin film with the TiO_2 anatase buffer layer exhibits highly a - and b -axis-oriented BIT single phases.

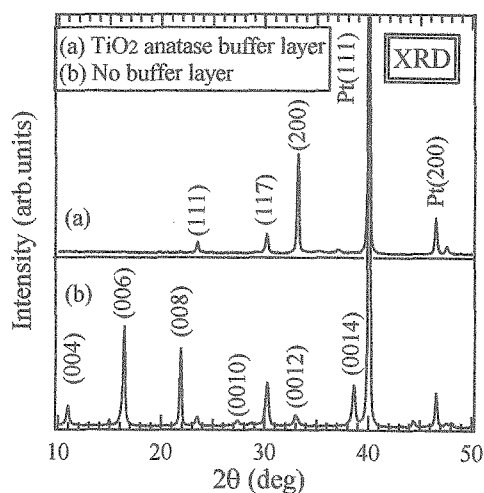


Fig. 1: XRD patterns of as-deposited BIT thin films with no buffer layer and with TiO_2 anatase buffer layer. The thicknesses of the buffer layer and the BIT thin film are fixed at 50 nm and 350 nm, respectively.

The mechanism of a - and b -axis orientation of the BIT thin film with the TiO_2 anatase buffer layer is very complicated. The lattice parameters of TiO_2 anatase are $a=0.378$ nm and $c=0.949$ nm. The interval of oxygen ion distribution along (101) of TiO_2 anatase is considered to be closer to the a - and b -axis lattice parameters (0.541 nm) than to the c -axis parameter (3.283 nm) of BIT. The lattice mismatch between BIT and TiO_2 anatase is estimated to be approximately 5.4%. However, this value is almost of the same order as the lattice mismatch between BIT and Pt. Therefore, the concept of lattice mismatch cannot explain the a - and b -axis orientation of the BIT thin film. This implies that the TiO_2 anatase buffer layer does not act as a simple barrier layer that prevents interdiffusion between the BIT thin film and the Pt substrate.

Figure 2 shows the cross-sectional micrographs of the BIT thin films with no buffer layer and with the TiO_2 anatase buffer layer. The BIT thin film with no buffer layer consists of well-developed grains with diameters of approximately 400 nm. The grains are isotropic and round. These micrographs indicate that one or two grains are stacked along the out-of-plane direction.

The surface and interface of the BIT thin film with the TiO_2 anatase buffer layer are very smooth, indicating that the interface structure between the BIT thin film and the Pt electrode is improved by introducing the TiO_2 anatase buffer layer. However, the TiO_2 anatase buffer layer disappears with the formation of the BIT thin film. These results may be evidence that the TiO_2 anatase buffer layer acts not as a barrier layer but as an initial nucleation layer of the BIT thin film.

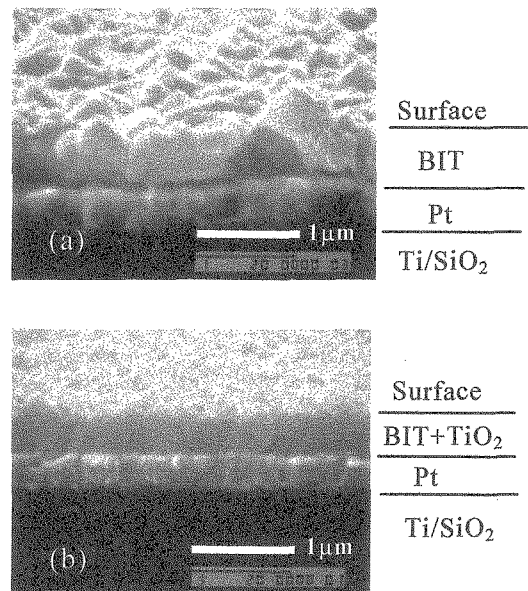


Fig. 2: SEM cross-sectional micrographs of as-deposited BIT thin films with (a) no buffer layer and with (b) TiO_2 anatase buffer layer.

Figure 3 shows the P - E hysteresis loops for the BIT thin films with no buffer layer and with the TiO_2 anatase buffer layer. These hysteresis loops exhibit good shape, although the saturated loops were not observed. The $2P_r$ of as-deposited BIT thin films with no buffer layer and that with the TiO_2 anatase buffer layer were $10.0 \mu\text{C}/\text{cm}^2$ and $44.4 \mu\text{C}/\text{cm}^2$, respectively. The $2E_c$ of as-deposited BIT thin films with no buffer layer and that with the TiO_2 anatase buffer layer were $233 \text{ kV}/\text{cm}$ and $300 \text{ kV}/\text{cm}$, respectively. The small P_r of as-deposited BIT thin film with no buffer layer originates from the highly c -axis orientation. The relatively large P_r of the as-deposited BIT thin film with the TiO_2 anatase buffer layer originates in the highly a - and b -axes orientations. However, the P_r of the a - and b -axes-oriented BIT thin film is smaller than that of the a -axis of the BIT single crystal. This originates from the existence of (111) and (117) peaks. The ϵ_r of the BIT thin film with no buffer layer and that with the TiO_2 anatase buffer layer were ~ 160 and ~ 300 , respectively. The leakage current (I_L) was $\sim 10^{-6} \text{ A}/\text{cm}^2$ in both BIT thin films. The I_L was not improved by the insertion of the TiO_2 anatase buffer layer. The large ϵ_r and I_L are considered to be due to the oxygen vacancy of the BIT thin film deposited on the TiO_2 anatase buffer layer, which has a small amount of oxygen vacancy.

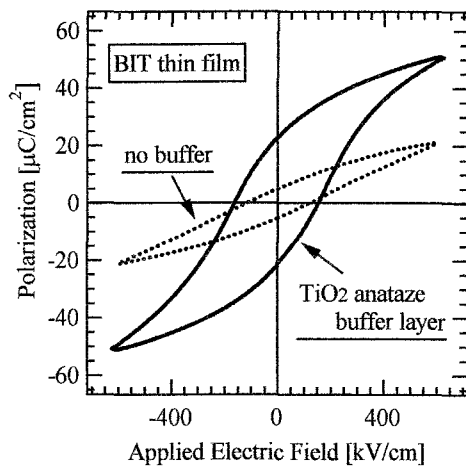


Fig. 3: P-E hysteresis loops of as-deposited BIT thin films with no buffer layer and with TiO₂ anatase buffer layer.

Figure 4 shows XRD patterns as a function of thickness of the as-deposited BIT thin film with the TiO₂ anatase buffer layer. The film thickness of the TiO₂ anatase buffer layer is fixed at 25 nm in order to prove the effect of the buffer layer on the BIT thin film. The XRD patterns were confirmed for the BIT thin film with thickness ranging from 80 to 550 nm. The composition ratios of Bi and Ti were almost stoichiometrical in the BIT thin films with thickness ranging from 80 to 400 nm. The XRD patterns of the BIT thin films with thickness ranging from 80 to 400 nm exhibit highly *a*- and *b*-axes-oriented BIT single phase. However, the pyrochlore phase shown as a closed circle is observed in the BIT thin films with thicknesses of 460 and 550 nm, since the composition ratios of these thin films are Bi-excess and Ti-poor. The existence of the Bi₂O₃ phase is attributed to the decrease in nucleation density of the TiO₂ anatase buffer layer with increasing in BIT thin film thickness, since the intensity of the Bi₂O₃ phase of 550 nm is larger than that of 460 nm. This is direct evidence that the TiO₂ anatase buffer layer acts as an initial nucleation of the BIT thin film.

Figure 5 shows P-E hysteresis loops as a function of thickness of the as-deposited BIT thin film with the TiO₂ anatase buffer layer. The P-E hysteresis loops are not observed in the BIT thin films with thicknesses of 460 and 550 nm, which exhibit the existence of the Bi₂O₃ phase. As the BIT film thickness increased, the hysteresis loop became square in shape. The E_c does not change much against the film thickness. A similar situation has been reported in the *c*-axis-oriented epitaxial BIT thin film and the PZT thin film [17,21,22]. When the low dielectric layer exists, it should strongly affect the E_c, particularly for thinner films. However, such an apparent change is not observed in this study. On the other hand, it is significant that the P_r value is found to be strongly dependent on the film thickness. The P_r value decreases with decreasing thickness of the BIT thin film. In particular, the low P_r and poor saturation of BIT thin films below 120 nm contribute to the remaining TiO₂ anatase buffer layer, which acts as

low dielectric layer. Therefore, the most suitable ratio of the thickness of the BIT thin film to the TiO₂ anatase buffer layer is considered to be [(BIT)/(TiO₂)] = 15, although the ratio may change with the thickness of the TiO₂ anatase buffer layer. To further investigate the mechanism of *a*- and *b*-axes orientation, ferroelectricity, and grain size of BIT thin film with TiO₂ Anatase buffer layer, the effect of film thickness of TiO₂ Anatase buffer layer and the detailed analysis of interface must be clarified in the future study.

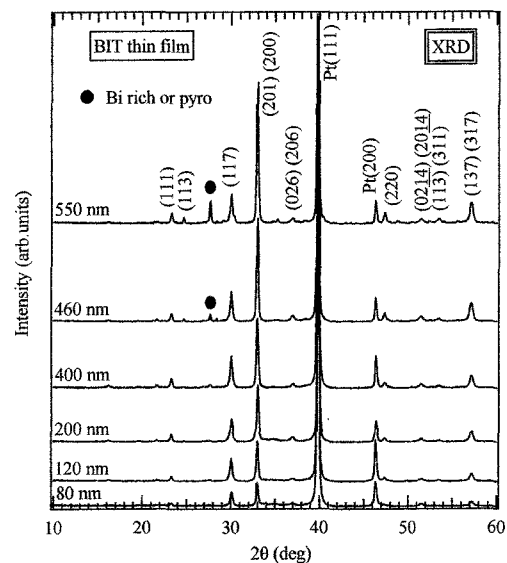


Fig. 4: XRD patterns as a function of thickness of as-deposited BIT thin films with TiO₂ anatase buffer layer.

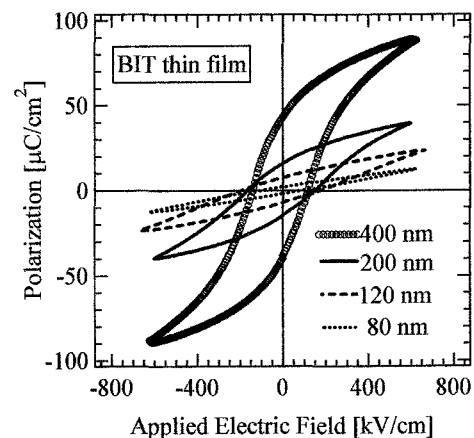


Fig. 5: P-E hysteresis loops as a function of thickness of as-deposited BIT thin films with the TiO₂ anatase buffer layer.

4. CONCLUSION

We have prepared *a*- and *b*-axes-oriented BIT thin films with the TiO₂ anatase buffer layer deposited on Pt/Ti/SiO₂/Si substrate using MOCVD technique. The BIT thin films were crystallized at the low-temperature of 500 °C. The BIT thin films with the TiO₂ anatase buffer layer exhibit highly *a*- and *b*-axes orientations.

The interface structure between the BIT thin film and the Pt electrode is improved by the TiO₂ anatase buffer layer. The BIT thin films with the TiO₂ anatase buffer layer exhibit relatively large P_r , which originates in the highly a - and b -axes orientations. When the film thickness was fixed at 400 nm, P_r and E_c were $2P_r = 81.6 \mu\text{C}/\text{cm}^2$ and $2E_c = 250 \text{ kV}/\text{cm}$, respectively. The dielectric constant (ϵ_r) was 160. The P_r and ϵ_r of the BIT thin film with the TiO₂ anatase buffer layer were almost of the same order as those along the a -axis of a BIT single crystal. These excellent ferroelectric and structural properties contribute the existence of the TiO₂ anatase buffer layer, which acts as an initial nucleation of the BIT thin film.

ACKNOWLEDGEMENT

This work was supported by a Grant- In-Aid for Scientific Research from the Ministry of Education, Culture, Sports, Science and Technology.

REFERENCES

- [1] S. E. Cummins and L. E. Cross: *J. Appl. Phys.* **39** (1968) 2268.
- [2] T. Takenaka and K. Sakata: *Jpn. J. Appl. Phys.* **19** (1980) 31.
- [3] R. Ramesh, K. Luther, B. Wilkens, D. L. Hart, E. Wang and J. M. Trascon: *Appl. Phys. Lett.* **57** (1990) 1505.
- [4] H. Esaki: *Integrat. Ferroelectr.* **14** (1997) 11.
- [5] T. Kijima, M. Ushikubo and H. Matsunaga: *Jpn. J. Appl. Phys.* **38** (1999) 127.
- [6] T. Kijima, S. Satoh, H. Matsunaga and M. Koba: *Jpn. J. Appl. Phys.* **35** (1996) 1246.
- [7] T. Kijima and H. Matsunaga: *Jpn. J. Appl. Phys.* **37** (1998) 5171.
- [8] T. Kijima and H. Ishiwara: *Jpn. J. Appl. Phys.* **41** (2002) L716.
- [9] T. Kijima and H. Matsunaga: *Jpn. J. Appl. Phys.* **38** (1999) 2281.
- [10] E. Tokumitsu, T. Isobe, T. Kijima and H. Ishiwara: *Jpn. J. Appl. Phys.* **40** (2001) 5576.
- [11] T. Kijima, Y. Fujisaki and H. Ishiwara: *Jpn. J. Appl. Phys.* **40** (2001) 2977.
- [12] M. Nakamura, T. Higuchi and T. Tsukamoto: *Jpn. J. Appl. Phys.* **42** (2003) 5687.
- [13] M. Nakamura, T. Higuchi and T. Tsukamoto: *Jpn. J. Appl. Phys.* **42** (2003) 5969.
- [14] M. Nakamura, T. Higuchi, Y. Hachisu and T. Tsukamoto: *Jpn. J. Appl. Phys.* **43** (2004) 1449.
- [15] T. Higuchi, M. Nakamura, Y. Hachisu, M. Saitoh, T. Hattori and T. Tsukamoto: *Jpn. J. Appl. Phys.* **43** (2004) 6585.
- [16] B. H. Park, B. S. Kang, S. D. Bu, T. W. Noh, J. Lee and W. Jo: *Nature* **410** (1999) 682.
- [17] U. Chon, G. Yi and H. M. Jang: *Appl. Phys. Lett.* **78** (2001) 658.
- [18] Y. Hou, X. Xu, H. Wang, M. Wang and S. Shang: *Appl. Phys. Lett.* **78** (2001) 1733.
- [19] T. Watanabe, H. Funakubo, M. Osada, Y. Noguchi and M. Miyayama: *Appl. Phys. Lett.* **80** (2002) 100.
- [20] T. Watanabe, A. Saiki, K. Saito and H. Funakubo: *J. Appl. Phys.* **89** (2001) 3934.
- [21] T. Watanabe, H. Funakubo, M. Mizuhira and M. Osada: *J. Appl. Phys.* **90** (2001) 6533.
- [22] T. Watanabe, H. Funakubo, K. Saito, T. Suzuki, M. Fujimoto, M. Osada, Y. Noguchi and M. Miyayama: *Appl. Phys. Lett.* **81** (2002) 1660.
- [23] H. Matsuda, S. Ito and T. Iijima: *Appl. Phys. Lett.* **83** (2003) 5023.
- [24] T. Kijima, Y. Kawashima, Y. Idemoto and H. Ishiwara: *Jpn. J. Appl. Phys.* **41** (2002) L1164.
- [25] T. Kijima and H. Ishiwara: *Jpn. J. Appl. Phys.* **42** (2003) L404.
- [26] M. K. Lee, Y. M. Hung and J. J. Huang: *Jpn. J. Appl. Phys.* **40** (2001) 6543.
- [27] E. K. Kim, M. H. Son, S. K. Min, Y. K. Han, C. H. Wang and S. S. Yom: *J. Appl. Phys.* **79** (1996) 4459.

(Received December 10, 2005; Accepted January 31, 2006)